DOI: 10.1002/anie.201100111

Nanomotors

Interaction of a Chemically Propelled Nanomotor with a Chemical Wave**

*Snigdha Thakur, Jiang-Xing Chen, and Raymond Kapral**

Dedicated to the Fritz Haber Institute, Berlin, on the occasion of its 100th anniversary

Self-propulsion on small scales is an ubiquitous phenomenon in biology. Bacteria and other microorganisms swim in order to obtain food or to respond to stimuli,[1] molecular motors like ATP synthase are the engines that power swimming motion,[2] and kinesin and other molecular motors are essential for active transport in the cell, participate in the DNA replication process and perform a variety of other essential tasks.[3,4]

More recently, there has been considerable interest in synthetic nano- and micrometer-scale self-propelled objects.[5,6] Chemists have fabricated a variety of nanomachines that either swim by unsymmetrical motions driven by external fields[7] or utilize chemical reactions to effect directed motion.[8–13] Theoretical models have been constructed to describe chemically powered nanomotors.[14–18] Several supramolecular entities, such as pseudorotaxanes, rotaxanes, and catenanes, that can be used as molecular switches,[19,20] molecular brakes, and rachets[21] have been developed. Synthetic nanomotors with no moving parts and use chemical energy for their directed motion provide some of the simplest examples of self-propulsion on nano- and micrometer scales. These include bimetallic nanorods,[8–11] Pt–silica sphere dimers,[12] and Janus particles.[13] There has also been a significant effort aimed at controlling the motion and transport of nanoscale objects by magnetic fields,[9,22–24] microchannel networks,[23] chemical sensing,[25] and other means. The interest in these synthetic nanomachines stems from their potential applications: targeted drug delivery, pick up and delivery of cargo, motion-based biosensing, nanoscale assembly, targeted synthesis, nano- and microfluidics, collective oscillations, nanoactuators, etc.[5,23–30]

It is well known that chemical systems which are displaced far from equilibrium may exhibit temporal oscillations and chaos or may self-organize to form spatially inhomogeneous patterns such as chemical waves in solution or on catalytic surfaces, Turing patterns, etc.[31] Questions that naturally arise are, how do nanomotors move and respond to chemically active environments, and can the inhomogeneity in the environment be used to influence the dynamics of motors and possibly provide a way to control their motions? Here, we consider how a sphere dimer motor moves in a chemically active medium and interacts with a chemical wave. We find that a chemical wave is able to reflect a dimer motor (Figure 1) and suggest that this effect can provide a possible mechanism for the control of nanomotor motion in a patterned chemical system. Our investigation provides an introduction to the broader issue of self-propulsion in active media and suggests the possibility of a new class of applications and control scenarios.

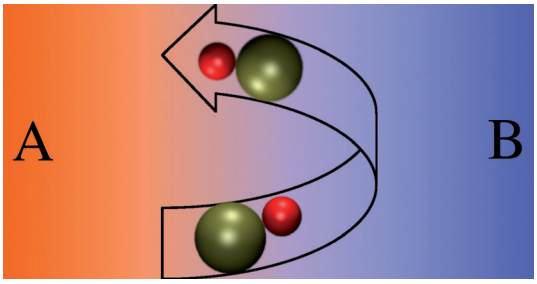

Figure 1. Trajectory of a self-propelled nanodimer motor showing the reflection from a chemical wave in a system with cubic autocatalysis involving *A* and *B* species.

We study the quasi-two-dimensional motion of a sphere dimer motor moving in a chemically active medium confined between two planes, so that the dynamics is similar to that in thin layers of solution or on active catalytic surfaces. The two confining planes are taken to be perpendicular to the z-axis and separated by a distance L_z. The nanomotor interacts with the confining planar walls through a 9–3 Lennard–Jones (LJ) potential[32] giving rise to quasi-two-dimensional motion in the xy-plane. While we study sphere dimer motors, the nanomotors may be spherical Janus particles or have more complicated shapes. The sphere dimer consists of linked catalytic (C) and noncatalytic (N) spherical monomers with a fixed internuclear separation R.[16,17,32] Our dimer motor model has been shown to capture many features of the

[*] S. Thakur, Prof. R. Kapral
Chemical Physics Theory Group, Department of Chemistry
University of Toronto, Toronto, Ontario M5S 3H6 (Canada)
E-mail: rkapral@chem.utoronto.ca
J.-X. Chen
Department of Physics, HangZhou Dianzi University
Hangzhou 310018 (China)

[**] This work was supported by a grant from the Natural Sciences and Engineering Research Council of Canada. Computations were performed on the GPC supercomputer at the SciNet HPC Consortium. SciNet is funded by the Canada Foundation for Innovation under the auspices of Compute Canada, the Government of Ontario, the Ontario Research Fund—Research Excellence, and the University of Toronto.

Supporting information for this article is available on the WWW under http://dx.doi.org/10.1002/anie.201000111.

dynamics of Pt–silica dimer motors, which have been studied experimentally.[12] The solution in which the nanomotor moves contains A and B particles, which interact with the walls through bounce-back collisions that reverse their velocities. These species interact with the nanodimer monomers through repulsive 6–12 LJ potentials, $V_{C\alpha}$ and $V_{N\alpha}$, $\alpha = A,B$. As in earlier studies of this model,[16] we assume that the A and B species interact with different potentials on the N monomer but have identical interactions with the C monomer. An irreversible chemical reaction, $A + C \rightarrow B + C$, occurs at the C sphere in the nanodimer and generates a nonequilibrium concentration gradient in the vicinity of the nanodimer. The nonequilibrium concentration gradient, in conjunction with the difference in the potential energy of the A and B particles with the N monomer, are responsible for the self-propulsion of our nanodimer.[16]

We suppose that solution in which the nanomotor moves is an active medium where the cubic autocatalytic reaction $B + 2A \xrightarrow{k_2} 3A$ takes place. Here k_2 is the rate constant of the reaction. If the system initially contains the autocatalyst, A, in part of the system and the fuel, B, in another part, a moving chemical front will form where the autocatalyst consumes the fuel. The iodate/arsenous acid system can be accurately modeled by such cubic autocatalysis and the chemical front dynamics has been investigated experimentally in this system.[33] The front instabilities of cubic autocatalytic fronts that develop when the diffusion coefficients of fuel and autocatalyst are different have been studied.[33–36] Here we consider the situation where the diffusion coefficients of the A and B species are the same and a stable propagating chemical front exists. The reaction–diffusion equation for the B species density field is,[36,37]

$$\frac{\partial n_B(\mathbf{r},t)}{\partial t} = D\nabla^2 n_B(\mathbf{r},t) - k_2 n_B(\mathbf{r},t) n_A^2(\mathbf{r},t) \qquad (1)$$

where D is the mutual diffusion coefficient. The equation for $n_A(\mathbf{r},t)$ is not independent and follows from number conservation $n_A(\mathbf{r},t) + n_B(\mathbf{r},t) = n_0$, assuming that the local total density fluctuations may be neglected. The chemical front may be determined from the solution of this equation in a frame moving with the front velocity, $u = x - ct$ and the result is,[34] $n_B(u) = n_0(1 + e^{-cu/D})^{-1}$, with the front speed given by $c = (Dk_2 n_0^2/2)^{1/2}$.

The investigations of nanomotor dynamics presented here employ a particle-based mesoscopic molecular dynamics (MD)-reactive multiparticle collision dynamics (RMPC) scheme.[38–40] The method is described in the Supporting Information. We used RMPC dynamics to simulate a planar chemical front in the system.[36] The chemical front was initiated by uniformly distributing A particles in the left side of the slab (for $0 \le x \le 50$) and B particles in the right side of the slab (for $50 \le x \le 100$). Starting from this initial condition, a reaction front will develop at the interface between A and B particles, and will move from left to right in the box in the x direction with velocity c, as the autocatalyst A consumes B. The rate constant k_2 was varied from 10^{-4} to 5×10^{-3} to simulate fronts with different velocities. Technical information related to the implementation of the method and examples of its applications are given in recent reviews[41,42] and references therein. Further simulation details are given in the Supporting Information.

Before describing how a sphere dimer motor interacts with a chemical front, we consider the response of a chemically inactive particle (same as the N monomer of the dimer) to such a front. It is well known that particles can respond to chemical gradients by diffuseophoretic mechanisms. For example, when a colloidal particle is placed in a fluid having a non-uniform concentration of solute molecules, it will migrate towards higher or lower concentration depending on whether the solute is attracted to or repelled from the particle's surface.[43,44] A chemical front has a sharp concentration profile and provides a source of inhomogeneity that can drive such motion. The main difference between motion driven by a chemical front and a simple concentration gradient is that the front, and therefore the source of the gradient, moves. Subsequently we shall see that it is important to distinguish the motion of chemically inactive particles in gradients from that of the interaction of autonomous self-propelled particles with chemical fronts.

A noncatalytic particle N placed near the front will respond to the concentration gradient since the A and B particle interaction potentials with N differ. For $10^{-4} < k_2 < 10^{-3}$, when the chemical wave has a small velocity, the N particle moves with a velocity that is the same as that of the chemical front. The velocity of the N particle (and the front) depends on its position in the front, which in turn is determined by its initial position with respect to the chemical wave. Figure 2a shows the x-component of the N particle

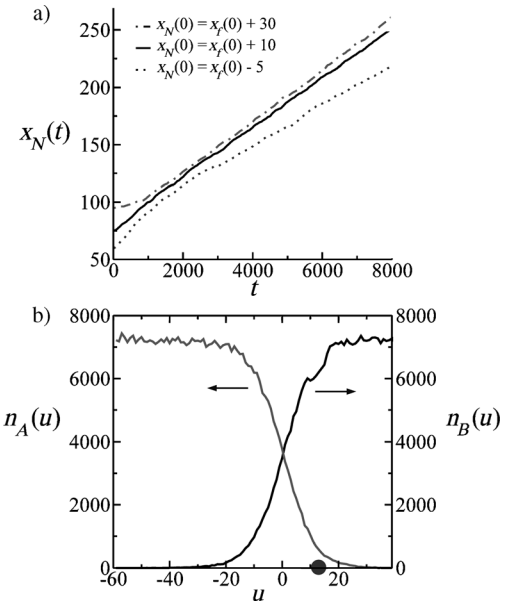

Figure 2. Chemically inactive particle N moving with the front for $k_2 = 10^{-4}$. a) Plot of $x_N(t)$ versus time for three different initial conditions indicated in the figure. b) Plot of the instantaneous wave profiles in a frame moving with the wave. The final position of the spherical particle in wave is depicted by the filled circle. The perturbation of the wave profile due to the presence of the N particle results in "kinks" in the profile seen in the figure. Quantities are given in simulation units (see the Supporting Information).

position, $x_N(t)$ as a function of time. Let $x_f(t)$ denote the position of the chemical front at the midpoint of the wave profile ($n_A(x_f(t)) = n_B(x_f(t))$) at time t. The initial position of the N particle was displaced relative to that of the front: $x_N(0) = x_f(0) + \delta$. The results of simulations with three different initial conditions are shown in Figure 2a: 1. $\delta = -5$, 2. $\delta = 10$, and 3. $\delta = 30$ (N particle completely in the B phase). From the slopes of the lines in Figure 2a one can see that the particle velocity depends on its initial position relative to the front. The calculated particle velocities for these cases are $V_x(\delta{=}{-}5) = 0.017$, $V_x(\delta{=}10) = 0.020$, and $V_x(\delta{=}30) = 0.022$. In all these cases, after a transient, the particle moves with the same velocity as the chemical wave. Figure 2b shows the front profile in a moving frame after transients have decayed; the steady-state position of the particle relative to the front is also shown. In the absence of a particle the chemical front moves with velocity $c = 0.022$, which agrees with the theoretical prediction from the reaction–diffusion equation given above [Equation (1)]. Depending on the initial condition, the presence of the particle can alter the chemical front velocity; for initial conditions where the particle resides completely in the B phase, so that the front approaches the particle and sets it in motion, the front velocity is indistinguishable from that when the particle is not present. For the other cases the steady-state location of the particle relative to the front depends on the initial condition, leading to a modification of the front velocity. By contrast, for larger rate constants, $k_2 > 10^{-3}$, the front velocity is large and the force provided by the concentration gradient is insufficient for the particle to move with the front; hence, the front moves forward in this case leaving the N particle behind.

The dynamics of a sphere dimer motor interacting with a chemical front differs considerably from that of a chemically inactive particle. The dimer itself catalyzes the reaction $A + C \rightarrow B + C$ so that it can move in a medium with only A particles and its velocity will be affected by the nature of the A and B particle local concentration fields in the vicinity of the front. To study the dynamics, we introduce the dimer in a spatial region having only A particles, with its catalytic side towards the chemical front (Figure 3a). The dimer moves toward the chemical wave with the C monomer at the front.

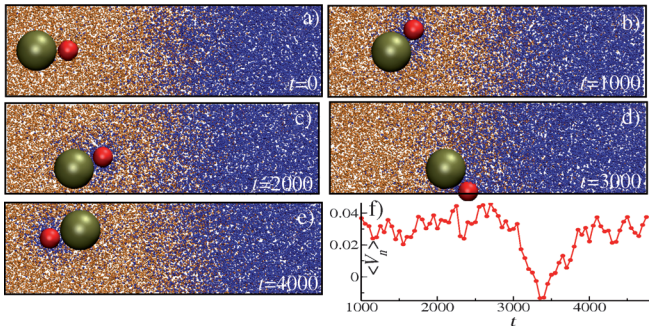

Figure 3. Dynamics of the self-propelled nanodimer in presence of a chemical wave front. Plots (a) to (e) show the instantaneous configuration of A (orange) and B (blue) molecules in the vicinity of the non-catalytic particle in a $40\times20\times2$ slice. The rate constant of the autocatalytic reaction is $k_2 = 10^{-4}$. Panel (f) shows the average center-of-mass velocity of the nanodimer $\langle V_n \rangle$ versus time.

Self-propelled nanomotors are subject to orientational fluctuations that give rise to diffusive motion on long enough scales. In applications where persistent directed motion is necessary, such as the interactions with chemical waves considered here, it is necessary to design motors where the orientational relaxation time is long compared to relevant time scales in the system. Otherwise a rapidly rotating motor would mask directed motion and be of little use for many applications. Our sphere dimer motor was constructed to have a long orientational relaxation time, $\tau_\theta = 3000$, so that, on average, it moves 20 times its length before reorientation occurs.

Figure 3a–e shows the trajectory of the dimer. For the conditions of this simulation, the dimer velocity along its bond, $V_n = 0.03$, is higher than the wave velocity, $c = 0.022$. Hence, the dimer is able to catch up with the chemical wave. The dimer cannot completely pass through the chemical wave since it would then find itself in a region without fuel for self-propulsion. Based on the simulation results for an inactive particle, one might anticipate that the dimer would then move with the chemical wave. However, once the dimer encounters the front, it senses the concentration gradient due to the chemical wave. In the absence of a chemical wave, the concentration gradient produced by the dimer that is responsible for the self propulsion is directed along the bond and is symmetric normal to the bond. The Brownian motion of the dimer in the presence of the chemical wave breaks this symmetry and induces forces that lead to reorientation of the dimer in the wave. Once the reorientation results in a configuration where the catalytic monomer is directed away from the front, the self-propulsion mechanism dominates and the dimer will move into the bulk A phase away from the wave. The sequence of panels in Figure 3 and a movie presented in the Supporting Information show the complete reorientation of dimer after encounter with the wave front. The last panel, Figure 3f, plots $\langle V_n \rangle$, the average of V_n over realizations, versus time in an ensemble of such trajectories. The decrease in $\langle V_n \rangle$ and its subsequent increase as seen in Figure 3f is due to the reorientation of dimer when it interacts with the chemical front. Immediately after reflection, the sphere dimer experiences a higher A particle concentration at the C end and a higher B concentration at the N end. Since $\varepsilon_A > \varepsilon_B$, this gives rise to a short period where the velocity of the dimer is negative (towards the N end). As the catalytic reaction at the C sphere occurs, the B particle concentration increases at the C end, restoring the positive velocity of dimer.

In order to investigate the robustness of such dimer dynamics, where a complete reflection of dimer occurs on its encounter with the wave, the initial condition of dimer was changed. In a system with an established chemical wave front, we introduce the dimer in a region having only B particles, with its catalytic side away from the wave front. Since the dimer is completely in the B phase to begin with, the catalytic reaction on the C monomer will not occur, the propulsion force will be zero and no directed motion will take place. Instead, the dimer will behave as a Brownian particle. The propagating chemical wave front will eventually collide with the dimer. On collision with the front, the dimer will

encounter *A* particles as a result of the concentration gradient. The dimer will then experience a gradient from both the chemical front and the reaction at the catalytic *C* monomer. As earlier, even a small asymmetry in the gradient is sufficient to reorient the dimer and cause it to move in the opposite direction. After reorientation, the dimer will move away from the chemical wave as in Figure 3e.

Figure 4 shows the trajectory of the dimer in the *xy* plane for the situation described above. The straight lines with different time labels denote the midpoint of the chemical wave at the indicated time instants. The left side of a line is the *A*-rich phase and right side is the *B*-rich phase. The time evolution of the dimer is labeled to match the chemical front at the same time instant. This representation allows one to see both the evolution of the chemical front and the self-propelled dimer in one figure. We again see the complete rotation of the dimer upon collision with the chemical wave; hence, a dimer moving in the same direction as the chemical front, regardless of its initial position in the system, will be reflected on collision with the wave. Reflection was also observed for dimers having a small orientational relaxation time, $\tau_\theta = 700$. This behavior differs from that of an inactive particle, which moves with the front after collision.

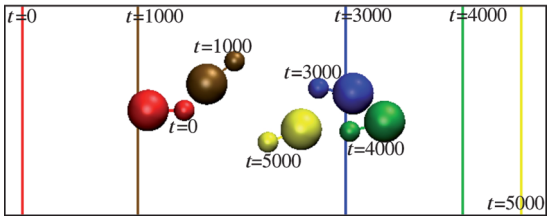

Figure 4. Trajectory of the nanodimer interacting with the chemical wave in *xy* plane for $k_2 = 10^{-4}$. Straight lines at different time steps denote the position of the midpoint of the chemical wave. At each time step the left side of the line has *A* particles while the right side has *B* particles. The positions of the dimer and chemical wave at the same time are denoted by the same color.

As suggested earlier,[18] we have shown that chemical waves can interact with inactive and self-propelled particles to influence their motion. The fact that chemically self-propelled particles can be reflected from chemical waves provides a possible means to control and target their motion. The propagating front considered in this study is a simple case that serves to illustrate the general principle. More interesting situations arise when one considers chemically patterned surfaces. It is well known that chemical patterns ranging from stationary regular and labyrinthine patterns to time-evolving structures can arise in chemical systems driven far from equilibrium. These patterns, in conjunction with the reflection mechanism described above, could be used to make self-propelled particles travel along prescribed paths, very much like the motion of nonbiological nanomotors in microchannels.[23] Furthermore, through long-range repulsive interactions patterns with nano- and micrometer-scale lengths[31,45] can be created which can serve to tightly control the dynamics of the nanomotors. The nature of the interaction between the nanomotor and chemical front can be altered by changing the catalytic reaction that powers the nanomotor and the reactions that lead to patterns in the chemically active medium. The full exploration of such applications will require further investigations of nanomotor propulsion mechanisms and the interactions of these motors with specific pattern-forming systems.

Received: January 6, 2011
Published online: March 23, 2011

Keywords: chemical waves · nanomotors · particle dimers · self-propulsion

[1] H. C. Berg, *E. coli in Motion*, Springer, New York, **2004**.
[2] P. D. Boyer, *Annu. Rev. Biochem.* **1997**, *66*, 717.
[3] R. D. Vale, R. A. Milligan, *Science* **2000**, *288*, 88.
[4] J. E. Molloy, C. Veigel, *Science* **2003**, *300*, 2045.
[5] E. Kay, D. Leigh, F. Zerbetto, *Angew. Chem.* **2007**, *119*, 72; *Angew. Chem. Int. Ed.* **2007**, *46*, 72.
[6] R. F. Ismagilov, A. Schwartz, N. Bowden, G. M. Whitesides, *Angew. Chem.* **2002**, *114*, 674; *Angew. Chem. Int. Ed.* **2002**, *41*, 652.
[7] R. Dreyfus, J. Baudry, M. L. Ropar, M. Fermigier, H. A. Stone, J. Bibetter, *Nature* **2005**, *437*, 862.
[8] W. F. Paxton, K. C. Kistler, C. C. Olmeda, A. Sen, S. K. S. Angelo, Y. Cao, T. E. Mallouk, P. E. Lammert, V. H. Crespi, *J. Am. Chem. Soc.* **2004**, *126*, 13424.
[9] T. R. Kline, W. F. Paxton, T. E. Mallouk, A. Sen, *Angew. Chem.* **2005**, *117*, 754; *Angew. Chem. Int. Ed.* **2005**, *44*, 744.
[10] W. F. Paxton, S. Sundararajan, T. E. Mallouk, A. Sen, *Angew. Chem.* **2006**, *118*, 5546; *Angew. Chem. Int. Ed.* **2006**, *45*, 5420.
[11] S. Fournier-Bidoz, A. C. Arsenault, I. Manners, G. A. Ozin, *Chem. Commun.* **2005**, 441.
[12] L. F. Valadares, Y.-G. Tao, N. S. Zacharia, V. Kitaev, F. Galembeck, R. Kapral, G. A. Ozin, *Small* **2010**, *6*, 565.
[13] H. Ke, S. Ye, R. L. Carroll, K. Showalter, *J. Phys. Chem. A* **2010**, *114*, 5462.
[14] R. Golestanian, T. B. Liverpool, A. Ajdari, *New J. Phys.* **2007**, *9*, 126.
[15] R. Golestanian, *Phys. Rev. Lett.* **2009**, *102*, 188305.
[16] G. Rückner, R. Kapral, *Phys. Rev. Lett.* **2007**, *98*, 150603.
[17] Y.-G. Tao, R. Kapral, *J. Chem. Phys.* **2008**, *128*, 164518.
[18] A. Mikhailov, D. Meinköhn, *Lect. Notes Phys.* **1997**, *484*, 334.
[19] V. Balzani, M. Gomez-Lopez, J. F. Stoddart, *Acc. Chem. Res.* **1998**, *31*, 405.
[20] J.-P. Sauvage, *Acc. Chem. Res.* **1998**, *31*, 611.
[21] T. R. Kelly, *Acc. Chem. Res.* **2001**, *34*, 514.
[22] W. F. Paxton, A. Sen, T. E. Mallouk, *Chem. Eur. J.* **2005**, *11*, 6462.
[23] J. Burdick, R. Laocharoensuk, P. M. Wheat, J. D. Posner, J. Wang, *J. Am. Chem. Soc.* **2008**, *130*, 8164.
[24] A. Ghosh, P. Fischer, *Nano Lett.* **2009**, *9*, 2243.
[25] D. Kagan, P. Calvo-Marzal, S. Balasubramanian, S. Sattayasamitsathit, K. M. Manesh, G.-U. Flechsig, J. Wang, *J. Am. Chem. Soc.* **2009**, *131*, 12082.
[26] S. P. Fletcher, F. Dumur, M. M. Pollard, B. L. Feringa, *Science* **2005**, *310*, 80.
[27] M. Alvarez-Pérez, S. M. Goldup, D. A. Leigh, A. M. Z. Slawin, *J. Am. Chem. Soc.* **2008**, *130*, 1836.
[28] S. Sundararajan, P. E. Lammert, A. W. Zudans, V. H. Crespi, A. Sen, *Nano Lett.* **2008**, *8*, 1271.
[29] M. E. Ibele, P. E. Lammert, V. H. Crespi, A. Sen, *ACS Nano* **2010**, *4*, 4845.
[30] T. Sakai, R. Yoshida, *Langmuir* **2004**, *20*, 1036.

[31] R. C. Desai, R. Kapral, *Dynamics of Self-organized and Self-assembled Structures*, Cambridge University Press, New York, **2009**.
[32] Y.-G. Tao, R. Kapral, *J. Chem. Phys.* **2009**, *131*, 024113.
[33] D. Horváth, V. Petrov, S. K. Scott, K. Showalter, *J. Chem. Phys.* **1993**, *98*, 6332.
[34] A. Malevanets, A. Careta, R. Kapral, *Phys. Rev. E* **1995**, *52*, 4724.
[35] R. A. Milton, S. K. Scott, *J. Chem. Phys.* **1995**, *102*, 5271.
[36] K. Tucci, R. Kapral, *J. Phys. Chem. B* **2005**, *109*, 21300.
[37] S. R. de Groot, P. Mazur, *Nonequilibrium Thermodynamics*, North-Holland, Amsterdam, **1962**.
[38] A. Malevanets, R. Kapral, *J. Chem. Phys.* **1999**, *110*, 8605.
[39] A. Malevanets, R. Kapral, *J. Chem. Phys.* **2000**, *112*, 72609.
[40] K. Rohlf, S. Fraser, R. Kapral, *Comput. Phys. Commun.* **2008**, *98*, 150603.
[41] R. Kapral, *Adv. Chem. Phys.* **2008**, *140*, 89.
[42] G. Gompper, T. Ihle, D. M. Kroll, R. G. Winkler, *Adv. Polym. Sci.* **2009**, *221*, 1.
[43] J. L. Anderson, M. E. Lowell, D. C. Prieve, *J. Fluid Mech.* **1982**, *117*, 107.
[44] H. J. Keh, Y. K. Wei, *Colloid Polym. Sci.* **2000**, *278*, 539.
[45] M. Hildebrand, M. Ipsen, A. S. Mikhailov, G. Ertl, *New J. Phys.* **2003**, *5*, 61.

